Optics and Lasers in Engineering 107 (2018) 202–206

Contents lists available at ScienceDirect

Optics and Lasers in Engineering

journal homepage: www.elsevier.com/locate/optlaseng

High sensitivity strain sensors based on single-mode-fiber core-offset Mach-Zehnder interferometers

Maria Susana Avila-Garcia[a], Marco Bianchetti[a,*], Ronan Le Corre[a,1], Alexis Guevel[a,1], Ruth Ivonne Mata-Chavez[a], Juan Manuel Sierra-Hernandez[b], Daniel Jauregui-Vazquez[b], José Roberto Reyes-Ayona[b], Julian Moises Estudillo-Ayala[b], Roberto Rojas-Laguna[b]

[a] *Departamento de Estudios Multidisciplinarios, Universidad de Guanajuato, Yuriria, Guanajuato 38944, Mexico*
[b] *Departamento de Ingeniería Electrónica, Universidad de Guanajuato, Salamanca, Guanajuato 36885, Mexico*

ARTICLE INFO

Keywords:
Mach–Zehnder
Interferometer
Strain sensor
Single mode fiber

ABSTRACT

Mach–Zehnder interferometers make highly sensitive sensors of physical quantities based on the accumulated phase difference between two or more optical paths. In this work, the application of single-mode-fiber core-offset Mach–Zehnder interferometers as strain sensors is reported. Three in-line modal Mach–Zehnder interferometers were manufactured by splicing three pieces of single mode fiber with well-defined offset and orientation of the cores and a well-defined length of its middle section. These interferometers were characterized as strain sensors, and a maximum sensitivity of 7.46 pm/με was obtained over the linear range 0–1754 με. Compared to other strain sensors, the ones reported in this work achieve a high sensitivity using inexpensive single mode fiber and an easy manufacturing process.

© 2018 Elsevier Ltd. All rights reserved.

1. Introduction

Light weight, neutrality to electromagnetic interferences, high sensitivity, chemical inertness, and the possibility to transmit information over long distances with minimal degradation are some of the advantages that optic sensors provide over electronic sensors.

In an in-line all-fiber modal interferometric sensor, coherent light travelling through a fiber optic core is coupled to the core and cladding modes of the interferometer's middle section. Here, the optical paths of the fiber modes are altered by the interaction with an external physical quantity, and then recouple in the last section of the interferometer generating an interference pattern that depends on the accumulated phase difference between the excited modes.

In this work, single-mode-fiber core-offset Mach–Zehnder interferometers (MZIs) are tested as strain sensors. Strain sensors have a wide range of applicability, for example, as structural health monitors in the manufacturing and building industry, in railways, tunnels, pipelines, etc.

Different types of fibers have been used to manufacture MZI strain sensors having a high and wide sensitivity range, but often the manufacturing process is complex or makes use of expensive fiber or equipment. For instance, in [1,2] very high sensitivities of 102 and 61.8 pm/με were obtained by using multi core fiber as the interferometer mid-section. In [3,4] high sensitivities of 6.8 and 5.75 pm/με were obtained using MZI with elaborated structures which are complex to manufacture. Sensitivity values of ∼3 pm/με can be obtained in MZI structures by inscribing the fiber using expensive equipment such as CO_2 lasers [5], by using fairly expensive photonic crystal fibers [6], or by relying on complex structures such as waist enlarged fibers, multiple fiber combination, or tapers [7–9].

Other types of interferometers can be used to obtain high sensitivities, such as the Fabry–Perot interferometer. For instance, in [10] two cascaded Fabry–Perot interferometers were used to obtain a sensitivity of 47.14 pm/με, and in [11] an air bubble introduced in a single mode fiber (SMF) was used as a Fabry–Perot interferometer where a sensitivity of 43.0 pm/με was reported.

In this paper, three in-line modal MZIs were characterized as strain sensors achieving a maximum sensitivity of 7.46 pm/με over the linear range 0-1754 με. The interferometers were manufactured by splicing three pieces of SMFs with a well-defined offset and orientation of the cores and a well-defined length of its middle section.

2. Sensor fabrication

Three different in-line MZIs were fabricated using an inexpensive Corning SMF-28 single mode fiber, with core diameter of 8.2 μm,

* Corresponding author.
E-mail address: mb@ugto.mx (M. Bianchetti).
1 Permanent address: Institut Supérieur de l'Électronique et du Numérique, 29200, Brest, France.

https://doi.org/10.1016/j.optlaseng.2018.02.008
Received 28 August 2017; Received in revised form 30 January 2018; Accepted 12 February 2018
0143-8166/© 2018 Elsevier Ltd. All rights reserved.

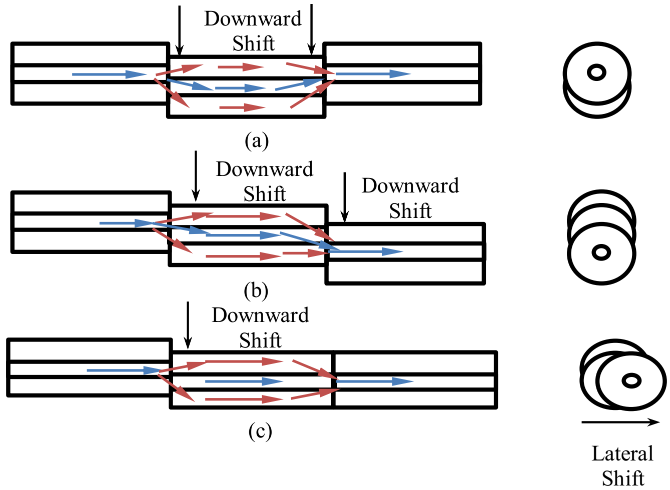

Fig. 1. Relative position of the three sections of the U, Z, and L interferometers. It also shows a schematic of the generation of the cladding modes (red) in the middle section and their recombination in the core mode (blue) of the third section. Fig. not to scale. (For interpretation of the references to color in this fig. legend, the reader is referred to the web version of this article.)

cladding of 125 μm, and coating of 245 μm. These interferometers are referred in the rest of the paper as U, Z, and L type as reported in [12].

The U type interferometer has a middle section that is shifted downwards by a fixed distance with respect to the first and third core-aligned sections, and as a result the three sections lay on the same plane, as illustrated in Fig. 1a. In the Z type interferometer, the middle and third sections are shifted downwards in the same direction by the same fixed distance and result coplanar, see Fig. 1b. In the L type interferometer, the middle section is shifted downwards, while the third section is shifted laterally with respect to the middle one. In this last case, the shifts are made in perpendicular direction one to another, so that the interferometer is not planar, see Fig. 1c. These geometries were previously proposed in [12–15], and in this work their characterization as strain sensors is reported. The details of the manufacturing process for these types of interferometers are reported in [12] where a Fujikura S175 splicer operated in manual mode was used. In this work though, the values of the splicing parameters were modified as follows: arc duration = 750 ms, arc energy = 91, cleaning time = 200 ms, pre fusion time = 240 ms, and z-push = 11 μm.

3. Principle of operation

In the Mach–Zehnder modal interferometers used in this work, several modes are excited at the first splice where the light travelling along the core of the first section is diffracted both in the cladding and in the core of the mid-section. After travelling through the mid-section, the modes re-join in the core of the third section at the second splice where they generate an interference pattern, as shown schematically in Fig. 1.

The phase difference between the core mode and a cladding mode is given by:

$$\Delta\varphi = 2\pi L \Delta n_e / \lambda \quad (1)$$

where, L is the distance between the splices, Δn_e is the difference in effective refractive index of the modes, and λ is the wavelength. The phase difference in (1) causes the interference to change between constructive and destructive fringes. The distance between consecutive fringes is given by $\Delta\lambda = \lambda^2 / L\Delta n_e$.

From these equations, it is clear that the fringe pattern will change if either the length, the effective refractive index difference, or both change. Both quantities can be affected by mechanical strain applied onto the interferometer.

Table 1
Interferometer geometry and contrast data.

Interferometer	Length [mm]	Core offset [μm]	Contrast [dBm]
L	15	10	~30
Z	10	10	~23
U	15	10	~27

In an interferometer a high fringe contrast (FC), i.e. the difference between consecutive minimum and maximum in the interference pattern, is due to the interference of modes with similar energy, and a high FC leads to a more precise and less noisy measurement.

4. Experimental setup

A schematic view of the strain system is illustrated in Fig. 2. A broad band light source (BBS) was set up using a 980 nm laser diode (QPhotonics diode QFBGLD 980-150) attached to wavelength division multiplexing WDM (Lightel 980/1585) and then connected to an Er doped fiber. The broad spectrum generated this way was then channeled into an interferometer. The interference pattern generated by the interferometer was measured with a Yokogawa AQ630B optical spectrum analyzer (OSA), in the range 1450–1650 nm with a resolution of 0.2 nm.

The interferometer was mounted across a fixed stage and a Thorlabs motorized travelling stage driven by a step motor controlled via a computer interface, see Fig. 2. The entire length of the interferometer was in-between the fixed and travelling stages, and fast drying glue was used to secure the fiber on the stages. The glue was applied on the coating of the fiber and the distance between the glued points was 114 mm for the all the interferometers. The travelling stage was moved for a maximum distance of 200 μm and returned to its initial position in steps of 10 μm. The maximum strain applied to the device was then ~1754 $\mu\varepsilon$ in steps of ~88 $\mu\varepsilon$.

5. Results and discussion

In order to find the optimal construction parameters, U, Z and L interferometers were manufactured with middle section lengths of 5, 10, 15, 20, 40, and 60 mm and core offsets of 5, 10, 15, and 20 μm. To be able to directly compare interferometers with the same geometry but different construction parameters, their interference patterns were analyzed while lying flat on an optical bench with an applied tension of 7.5 g. Interferometers with the highest FC were selected to be fully characterized, the construction parameters for these interferometers are listed in Table 1.

When the interferometers were mounted on the fixed and travelling stages, care was taken not to twist the interferometer, and a tension of 7.5 g was applied to have the same condition for each interferometer at the beginning of the experiment. Their interference spectrum was acquired in the range 1450–1650 nm, and their interference at 0 $\mu\varepsilon$ is shown in Fig. 3.

The interferometric patterns of the selected interferometers were acquired as strain was applied to the sensor, and then the shift of all interferometric dips was analyzed. The dip shifts with the highest sensitivity, widest measurement range and lowest data hysteresis were D_{L1}, D_{L2}, D_{Z1}, D_{Z2}, and D_U and are shown in Fig. 3. The behavior of these dips is shown in Figs. 4–6, where a full symbol reports the forward measurement, and an empty symbol reports the return measurement. It can be observed that the hysteresis, defined as $\max_i(F(S_i) - R(S_i))/F(S_i)$, where F and R are the forward and return measurement at strain S_i, is small, confirming the effectiveness of our measurement method.

In Fig. 4(a) and (b) the data for the D_{L1} and D_{L2} dips of the L type interferometer are shown. In this case, both dips shift in a non-linear manner with the applied strain, as confirmed with the good parabolic fit. Their average sensitivity is 4.2 and 4.5 pm/$\mu\varepsilon$, as obtained with a

Download English Version:

https://daneshyari.com/en/article/7131768

Download Persian Version:

https://daneshyari.com/article/7131768

Daneshyari.com